



Impact of the prequench state of binary fluid mixtures on surface-directed spinodal decompositionAbheeti Goyal ^{*}

*Fluids and Flows Group, Department of Applied Physics, Eindhoven University of Technology,
P.O. Box 513, 5600 MB Eindhoven, The Netherlands*
*and Theory of Polymers and Soft Matter Group, Department of Applied Physics, Eindhoven University of Technology,
P.O. Box 513, 5600 MB Eindhoven, The Netherlands*

Paul van der Schoot 

*Theory of Polymers and Soft Matter Group, Department of Applied Physics, Eindhoven University of Technology,
P.O. Box 513, 5600 MB Eindhoven, The Netherlands*

Federico Toschi 

*Fluids and Flows Group, Department of Applied Physics, Eindhoven University of Technology,
P.O. Box 513, 5600 MB Eindhoven, The Netherlands*



(Received 31 December 2020; accepted 18 March 2021; published 6 April 2021)

Using lattice Boltzmann simulations we investigate the impact of the amplitude of concentration fluctuations in binary fluid mixtures prior to demixing when in contact with a surface that is preferentially wet by one of the components. We find a bicontinuous structure near the surface for an initial, prequench state of the mixture close to the critical point where the amplitude of concentration fluctuations is large. In contrast, if the initial state of the mixture is not near the critical point and concentration fluctuations are relatively weak, then the morphology is not bicontinuous but remains layered until the very late stages of coarsening. In both cases, it is the morphology of a depletion layer rich in the nonpreferred component that dictates the growth exponent of the thickness of the fluid layer that is in direct contact with the substrate. In the early stages of demixing, we find a growth exponent consistent with a value of $1/4$ for a prequench state away from the critical point, which is different from the usual diffusive scaling exponent of $1/3$ that we recover for a prequench state close to the critical point. We attribute this to the structure of a depletion layer that is penetrated by *tubes* of the preferred fluid, connecting the wetting layer to the bulk fluid even in the early stages if the initial state is characterized by concentration fluctuations that are large in amplitude. Furthermore, we find that in the late stages of demixing the flow through these tubes results in significant in-plane concentration variations near the substrate, leading to dropletlike structures with a concentration lower than the average concentration in the wetting layer. This causes a deceleration in the growth of the wetting layer in the very late stages of the demixing. Irrespective of the prequench state of the mixture, the late stages of the demixing process produce the same growth law for the layer thickness, with a scaling exponent of unity usually associated with the impact of hydrodynamic flow fields.

DOI: [10.1103/PhysRevE.103.042801](https://doi.org/10.1103/PhysRevE.103.042801)**I. INTRODUCTION**

The kinetics of phase separation in binary fluid mixtures has attracted interest in the scientific community for a very long time, yet many aspects of this process remain unclear. For example, what precisely the impact is of hydrodynamics, thermal fluctuations, the quenching protocol, or the presence of a confining surface, is not all that well understood in spite of all this attention [1]. Apart from scientific interest, the theoretical investigation of phase separation kinetics is currently also inspired by a wide range of technological applications that include membrane fabrication and plastic electronics such as organic photovoltaics [2–6]. These require a detailed understanding of the demixing process under a variety of conditions, if the morphology of the mixture is to be

tailored before solidification of the fluid sets in. Most of the focus in this field is on determining the growth mechanisms following a so-called quench, in which the thermodynamic conditions of the fluid mixture are suddenly changed. These depend critically on whether the demixing is taking place in bulk, so away from the impact of any physical boundary, or whether it is taking place in the vicinity of a substrate, especially if that substrate is preferentially wet by one of the components of the mixture.

If a binary mixture is quenched in the *spinodal* region of the phase diagram, where the mixture is thermodynamically absolutely unstable, then phase separation occurs in a process known as *spinodal decomposition* and subsequently followed by *coarsening* [7–15]. In the early stages of spinodal decomposition, a scattering peak emerges due to the selective amplification of concentration fluctuations with a characteristic length scale. Once the two phases more or less attain their respective equilibrium concentrations, the peak shifts

^{*}a.goyal@tue.nl

toward smaller wave vectors with time, indicating the removal of the interfacial area by coarsening of the structure that has emerged. The characteristic domain size both in bulk mixtures and in mixtures in contact with preferentially wetting surfaces follows a power law with a growth exponent that itself, in fact, depends on time and represents the different prevalent subsequent coarsening mechanisms at play.

In bulk, the domain growth is isotropic whereas in mixtures in contact with a preferentially wetting surface, the interplay between bulk phase separation and wetting kinetics at the surface leads to anisotropic domain growth. This phenomenon is commonly referred to as *surface-directed spinodal decomposition*, and has been studied extensively in experiments [16–18] and simulations [19–28]. It is well-established that the preferentially wetting surface gives rise to a concentration wave which consists of alternating wetting and depletion layers of the preferred component. In this case the characteristic length scale is the width of the first wetting layer right next to the surface. However, the growth dynamics and hence the growth exponent of the characteristic length scale may depend, in principle, on the conditions such as the composition of the mixture, the quench depth, the thickness of the film and the initial structure of the mixture immediately before quench [15–32]. Out of these different influencing factors, the structure of the blend prior to the quench has so far received only limited attention [15,31].

The structure of the blend before the quench refers to the amplitude and spatial correlations of the concentration fluctuations that characterise the otherwise homogeneous mixture before it is suddenly brought out of thermodynamic equilibrium. Near to the critical point of the blend, concentration fluctuations are large in magnitude and correlations carry further in space than when the blend occupies a state further away from the critical point in the phase diagram. Remarkably, although there is experimental evidence of the influence of the prequench state on the onset of coarsening in demixing fluids [15], relatively little work has been done to investigate this systematically, theoretically nor experimentally [33,34]. In order to remedy this state of affairs, we shed light in this work on how the thermodynamic state of the blend prior to the quench impacts upon the growth dynamics, in particular if the fluid is in contact with a preferentially adsorbing surface. For this purpose, we make use of lattice Boltzmann simulations that take full account of the impact of hydrodynamics. As we shall see, both the structure and the time evolution of that structure, as well as the impact of hydrodynamics, are strongly affected by the initial state of the mixture. Hydrodynamics, in particular, plays a significant role from early times on, resulting in a faster domain growth for a prequench state close to the critical point, both in bulk mixtures and in mixtures in contact with preferentially wetting surfaces.

We model the impact of equilibrium concentration fluctuations by imposing them in the starting configurations of our simulations, where we compare the behavior of bulk mixtures and mixtures in contact with a surface that is preferentially wet by one of the components. For simplicity, we impose only the amplitude of these fluctuations and presume them to be randomly correlated in space, that is, uncorrelated between the grid points of our simulation box that represent a mesoscopic volumes of fluid. Hence, we ignore the exponential decay

away from the critical point and the algebraic decay at the critical point, realizing that high wave-number fluctuations are anyway penalized very strongly in the simulation and relax swiftly. Even with this simplification, we recover the influence of the prequench state on demixing in bulk found experimentally [15].

We find that in *bulk*, large initial concentration fluctuations accelerate the demixing process, leading to isotropic coarsening from the early times of the process onward. As reported in experimental studies for various prequench states of the bulk mixture [15], the onset of coarsening occurs at earlier times for a prequench state close to the critical point, and the growth exponents associated with the coarsening that we find turn out to not depend on the corresponding amplitude of the concentrations fluctuations in the initial state. Indeed, independent of the amplitude of the initial concentration fluctuations the demixing initiates via a spinodal mode wherein the peak in the structure factor remains stationary at a characteristic wave number for a while, after which it shifts toward lower values due to coarsening setting in. This then leads to domain growth with an exponent of unity.

In the vicinity of a substrate that prefers to be in contact with one of the two components of the mixture, we do find a growth exponent of the relevant length scale that depends on the prequench state of the mixture. The relevant length scale is, in that case, associated with the width of the wetting layer, rich in the preferred component. For large initial concentration fluctuations, implying a prequench state close to the critical point, we recover the usual Lifshitz-Slyosov-Wagner [35] diffusive growth exponent of $1/3$ followed by a viscous hydrodynamic regime exponent of 1 [10–14]. If we impose weak initial concentration fluctuations, then we find in clear contrast to this a growth exponent consistent with a value of $1/4$. This matches the growth exponent we obtain if we impose no concentration fluctuations prior to the quench, and start off with a perfectly uniform mixture. For the latter, we do not find the late-stage exponent of unity that we find for the former, as these are driven by Marangoni-type flows linked to curved interfaces that cannot develop in the absence of some level of structural inhomogeneity. Parenthetically, the scaling exponent $1/4$ is consistent with an interface-limited growth of a wetting film predicted by time-dependent Ginzburg–Landau-type models [36].

The different growth exponents that we find for small and large amplitudes of the zero-time fluctuations are associated with different local morphologies that form. Close to the substrate, we find a layered morphology for weak prequench concentration fluctuations and a bicontinuous one for large initial concentration fluctuations. For large prequench fluctuations, the depletion layer next to the wetting layer is penetrated by *tubes* of the preferred fluid, connecting the wetting layer to the bulk mixture from the early stages of demixing onward. These tubes accelerate the growth of the wetting layer. For small prequench fluctuations, however, these tubes form only in the later stages of the demixing, resulting in a delayed crossover to the viscous hydrodynamic coarsening regime.

Our simulations reveal that for a prequench state close to the critical point, the surface-tension-assisted hydrodynamic flow of preferred fluid through the depletion layer occurs

essentially from the start of the demixing process. In the late stages, however, the flow of fluid from bulk to the wetting layer through the tubes results in significant in-plane concentration variation in the wetting layer, and dropletlike structures with a smaller concentration of the wetting phase form on the substrate. This causes a temporary deceleration in the growth of the wetting layer. We believe that these findings can help rationalize the dynamics of demixing in the presence of a wetting substrate, and help optimize structural morphologies in the production of thin films.

The remainder of this paper is organized as follows. In Sec. II, we describe our model to simulate phase separation in binary mixtures, and how we implement the surface interaction and different amplitudes of the initial concentration fluctuations. The simulation results are presented and discussed in Sec. III. Finally, we conclude this paper with a summary in Sec. IV.

II. MODELING AND SIMULATION DETAILS

We make use of lattice Boltzmann (LB) model simulations to investigate the structural evolution of binary fluid mixtures, in bulk and in contact with a substrate. Lattice Boltzmann models are widely used in the studies of phase-separating fluids, owing to their ease to handle multicomponent fluids and providing an efficient description of hydrodynamic flow fields in such fluids [37–40]. In our implementation of the lattice Boltzmann framework, we introduce the interactions between the fluid components driving the phase-separation by means of the Shan-Chen pseudopotential method [39,40]. We implement surface interactions by means of a boundary condition at one boundary of our cubic computational domain, wherein the fluid density field at that boundary is used to control the strength of the fluid-solid interaction and parametrize the equilibrium contact angle. The method has been validated extensively, and allows for the investigation of a wide spectrum of substrate interaction strengths that we denote by φ [41,42]. For a quick introduction to the lattice Boltzmann method, the numerical implementation of the interaction of the fluids with substrate, and the simulation parameters, we refer to Appendix A.

For all our simulations, we use a cubic computational domain consisting of 256^3 grid points, representing an incompressible binary fluid mixture of components A and B with number densities ρ_A and ρ_B . The corresponding volume fractions are ϕ_A and ϕ_B . For definiteness and simplicity we assume a symmetric mixture with equal volume fractions, so $\phi_A = \phi_B = 0.5$ corresponding to the critical volume fraction in our simulations. We initialize the densities ρ_A and ρ_B such that the initial order parameter field ψ , defined as $\psi \equiv (\rho_B - \rho_A)/(\rho_B + \rho_A) \equiv \phi_A - \phi_B$, has a random spatial distribution of values $\pm\psi_0$. The amplitude $\alpha \in [0, 100]$ of the fluctuation we relate to the binodal (equilibrium) values of order parameter in the coexisting phases $\pm\psi_b$, via the definition $\psi_0 \equiv \alpha \times 10^{-2} |\psi_b|$. A large amplitude α of the initial concentration fluctuations mimics a state of the mixture near the critical point right before the quench [15,43]. If $\alpha = 0$, then we initialize the simulation with a homogeneous density distribution.

We report all the simulation parameters in lattice Boltzmann units [37]. The ratio G/G_{cr} of the value of the Shan-Chen [39] interaction potential right after the quench, G , and that at the critical point, G_{cr} , can be interpreted as the ratio of the corresponding Flory-Huggins interaction parameters, we set at a value of 1.18. This yields for the binodals $\rho_A = 0.4 = 1.2 - \rho_B$ and $\rho_B = 2.0 = 1.2 - \rho_A$, implying that $\psi_b = \pm 2/3$ [40]. A phase diagram of the Shan-Chen fluid can be found in Refs. [41,44]. Hence, the quench is rather deep, corresponding in temperature to, say, a sudden temperature drop of up to tens of Kelvin. The kinematic viscosity of both the fluids we fix at $\nu = 5 \times 10^{-3}$ [45].

In order to model demixing on a preferentially wetting substrate, the value of surface interaction at the bottom and top boundaries we set to $\varphi = 0.3$ and $\varphi = 0.0$. The latter choice leads to a neutral wall boundary condition at the top surface of the simulation box, that is, it has a neutral affinity for both the components. This we do to recover bulk behavior away from the substrate and to avoid any coupling of wetting effects from opposite walls. A value of $\varphi = 0.3$ at the substrate boundary should in equilibrium lead to partial wetting of a sessile drop of a B -rich phase on the substrate with 60 deg contact angle. At the remaining four boundaries of our simulation box we impose periodic boundary conditions.

Even though our choice of value of the contact potential φ should lead to partial wetting of the phase with the majority component B at the surface, the finite size of the domain in our simulations and the condensation of material at the substrate do lead to complete wetting within our simulation times. We note that we do not vary the strength of surface interaction in this work, because in a recent study we show that the characteristic length scale remains unaffected by its value within the ranges of 0.1–0.5 studied, both in the early and in the late stages of coarsening [44].

In this work, we model demixing with the amplitudes of the initial concentration inhomogeneities ranging between $\alpha = 0$ and 100. Particularly, we focus on the extreme amplitudes of strong initial concentration variations with $\alpha = 100$, and weak ones with $\alpha = 0$ and 1. Again, a value of $\alpha = 0$ corresponds to a scenario where there are no concentration fluctuations in the mixture at time zero, and all the grid points are initialized with the critical densities of the two components. In this case, the mixture needs an external stimulus, such as the presence of a preferentially wetting wall, to explore the energy landscape and initiate phase separation. Apart from $\alpha = 0$, we consider many different values between $\alpha = 1$ and 100. As we find from our simulations on bulk demixing, the extreme values of $\alpha = 1$ and 100 represent a prequench state relatively far away and close to the critical point of the mixture, respectively.

It is important to note that we do not include in our numerical model the role of thermal fluctuations *during* the demixing process. These thermal fluctuations are often modeled at the hydrodynamic level in terms of fluctuating hydrodynamics [46] in the lattice Boltzmann model [47]. While these fluctuations could potentially produce some influence on the dynamics of multicomponent fluids [48], these are not of interest for our study that is mostly focusing on the influence of a large quench.

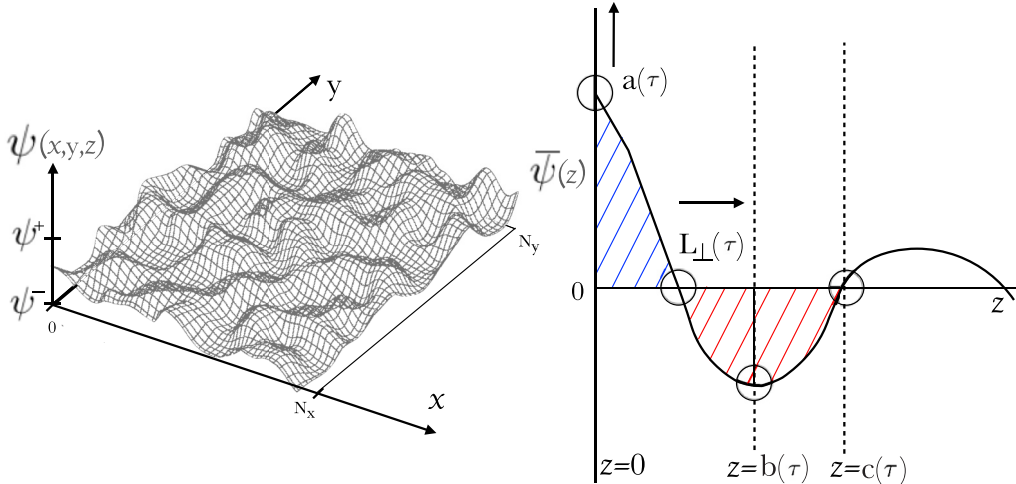


FIG. 1. (left) Sketch of the order parameter field $\psi(x, y, z)$ in a plane at a distance z away from the substrate at some time τ . The maximum and minimum values of the order parameter in the field are indicated by ψ^+ and ψ^- , respectively. To estimate the characteristic length scale normal to the substrate, the order parameter is laterally averaged over each plane parallel to the substrate. (right) Sketch of the in-plane average profile of the order parameter, $\bar{\psi}(z)$. The contact value of the order parameter we denote $a(\tau) = \bar{\psi}(0, \tau)$, which is a function of the time τ . The position of the first zero crossing of the order parameter we define as the wetting layer thickness $L_{\perp}(\tau)$, and the position of the plane half way between the first and second zero crossing at $c(\tau)$ we denote by $b(\tau)$. The front propagates toward the bulk, to a higher distance z , resulting in an increase of the layer thickness $L_{\perp}(\tau)$. The area shaded in blue indicates the wetting domain, that shaded in red a the primary depletion zone, poor in the wetting component.

Further, we scale the simulation time by the spinodal time scale, which is the time at which the peak in the structure factor starts to move toward a lower wave number. We obtain this time from our lattice Boltzmann simulations on bulk demixing in a simulation box with periodic boundary conditions in all directions [15], for which we set $\alpha = 100$. We choose this time as among the various values of α we investigate, it is the fastest relevant timescale in a bulk mixture. Results of these simulations are elaborated on at the end of the main text and are captioned as Appendix B.

Finally, the bulk length L and the in-plane length scale $L_{\parallel}(z)$ we estimate from the first moment of the (in-plane) structure factor [45], while the normal length scale, L_{\perp} , that we identify corresponds to the first zero crossing of the order parameter $\psi = \psi(z)$, laterally averaged over each plane parallel to the substrate; see Fig. 1. The characteristic length scales are presented in the units of the lattice size.

The prevalent bulk length scale we estimate from the position of the peak of the structure factor, allowing us also to clearly pinpoint the onset of coarsening, which happens when it starts to shift to a lower wave number. For bulk systems, we find the growth exponents associated with coarsening to be independent of the amplitude of the concentration fluctuations at zero time, as expected. The same is true for the morphology, showing that the white noise that we use to describe the equilibrium fluctuations in the prequench state does not alter the structure of the demixing bulk fluid reference.

III. RESULTS AND DISCUSSION

Before presenting a more quantitative discussion of our results, we first show representative snapshots of morphologies that develop with time, when a thermodynamically

unstable binary fluid mixture is in contact with a substrate that preferentially attracts one of the two fluids. Figure 2 shows images of a two-dimensional cut through the order parameter field $\psi = \psi(x, y, z)$ of a phase separating symmetric fluid AB mixture on a substrate that is preferentially wet by B in the xz plane, for different times τ . For a homogeneous initial condition $\alpha = 0$ (top row), alternate layers of fluid rich and poor in the preferred component form. At the surface, we have a layer rich in component B , next to it a layer poor in B and rich in A , next to that one poor in A rich in B , and so on. The number of such alternating layers rich and poor in B increases with time. The first layer rich in B we call the *wetting layer*, and the next layer rich in A but poor in B we call the *depletion layer*.

For $\alpha = 1$, representing one percent fluctuations in the background mixture composition at time zero, a morphology resembling that of the case $\alpha = 0$ forms in the early stages of demixing. However, as shown in the middle row of Fig. 2, the layers are less well defined and break up to slowly form an interconnected morphology in the later stages of the demixing. We can clearly see the development of the wetting layer and the depletion layer that both increase in width with time. The depletion layer is the last to break up to connect the wetting layer to a layer rich in B , allowing for the wetting layer to grow wider faster. Note that this layer connects to the mixture further away from the substrate that resembles in structure and predominant length scale a bulk system.

For very large amplitude of fluctuations $\alpha = 100$ (bottom row), the stratified structure never forms. The wetting layer does form and remains intact while the depletion layer that develops exhibits *holes* or *tubes* from the early times on, connecting the wetting layer to what resembles the interconnected morphology of a bulk fluid in the process of demixing and

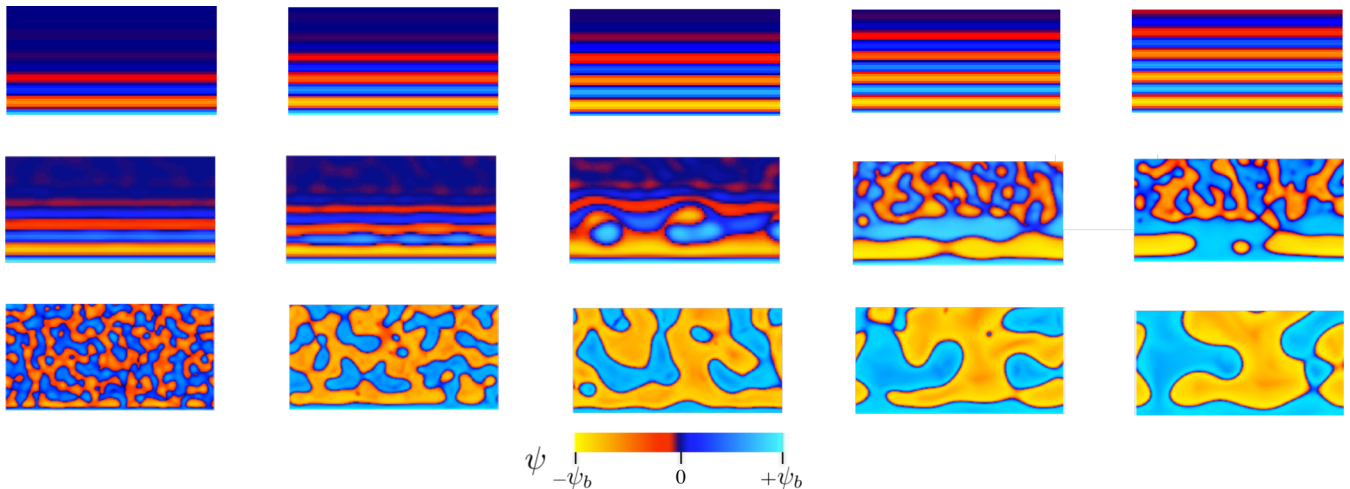


FIG. 2. Snapshots of the morphology resulting from the phase separation of a symmetric fluid mixture in the central plane normal to the substrate that is situated at the bottom of the panels. Time runs from left to right for three amplitudes of concentration fluctuations (from top to bottom). For the amplitudes of the initial concentration fluctuations, we set $\alpha = 0$ (top row), 1 (middle row), and 100 (bottom row). Snapshots are shown at dimensionless times $\tau = 4, 8, 12, 16,$ and 20 from left to right. The time τ is simulation time scaled by the spinodal time that we obtain from a bulk simulation, initialized with $\alpha = 100$. As is clearly visible, substrate wetting leads to the formation of horizontal patterns and of a B-rich layer (the “wetting layer”), immediately in contact with the substrate and present for all values of α . The B-rich regions with positive order parameter $\psi > 0$ are shown in blue, while the yellow regions with $\psi < 0$ show the A-rich phase. The binodal (equilibrium) value of the order parameter in the coexisting phases is denoted by ψ_b , and has a value of $2/3$. See the main text for details.

coarsening. No obvious coarsening takes place in the usual sense if we set $\alpha = 0$, albeit the wetting layer does increase in width with time via diffusion of the wetting component B across the depletion layer. This is a slow process, for the wetting component has to traverse the depletion layer that acts as a thermodynamic barrier.

To quantify the morphological evolution of the demixing fluid near a substrate, we need to measure two quantities rather than one on account of the broken symmetry imposed by the presence of the substrate. We identify as relevant length scales the wetting layer thickness, L_{\perp} , and the in-plane length scale, $L_{\parallel}(z)$, which depends on the distance z from the substrate. We recall (i) that we identify L_{\perp} as the first zero crossing of the order parameter profile $\psi(z)$ and can be seen as the wetting layer thickness, and (ii) that we obtain $L_{\parallel}(z)$ from the first moment of the in-plane structure factor [45]. Figure 3 shows the time evolution of the normal length scale L_{\perp} for fluctuation amplitudes α in the range from 0 to 100. For a prequench state mimicking one close to the critical point, with a large value of α , we seem to recover the exponents $1/3$ and 1 in the early and the late stages of demixing, respectively. These are the values we expect for diffusive and viscous hydrodynamic coarsening [7]. For a prequench state away from the critical point corresponding to $\alpha = 1$, however, we find a scaling exponent that seems closer to $1/4$ than $1/3$ in the early stages of demixing, crossing over to a value of 1 much later in time. An exponent of $1/4$ matches that obtained from the wetting layer thickness for $\alpha = 0$, consistent with an interface-limited growth of a wetting film predicted theoretically [36]. This indicates that for early times, the demixing in mixtures away from the critical point is dominated by surface effects. This, in fact, is also what we expect from the snapshots of Fig. 2, namely, that weak fluctuations do not initially destroy the stratified layer structure, only make it less well defined.

The transition to a power law with exponent larger than $1/4$ we find to correspond with the break up of the secondary wetting layer, that is, the layer next to the depletion layer

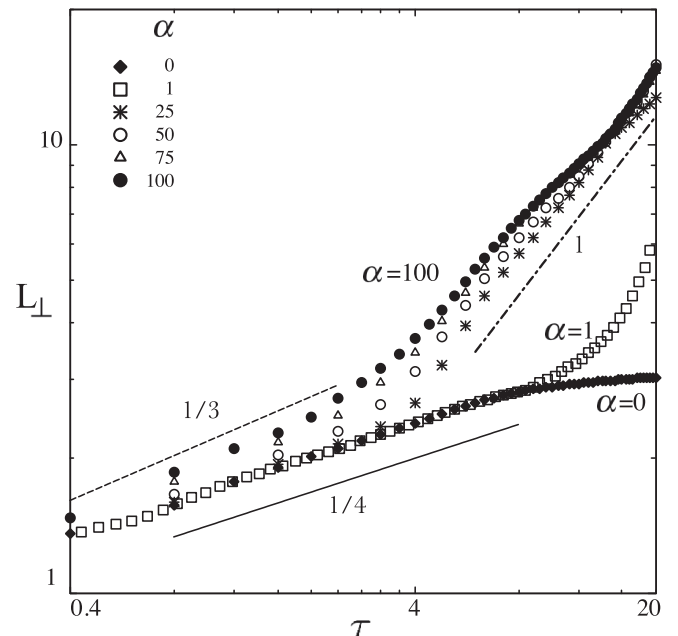


FIG. 3. Time dependence of the characteristic length scale L_{\perp} normal to the substrate. The symbols represent different amplitudes of the initial concentration variations, ranging between $\alpha = 0$ and 100. A larger amplitude indicates a *prequench* state of the mixture closer to the critical point. Shown for comparison are also scaling exponents of $1/3$, $1/4$, and 1 . The time τ is scaled to the spinodal time corresponding to the bulk mixture initialized with $\alpha = 100$, obtained from a separate simulation [44]. See also the main text.

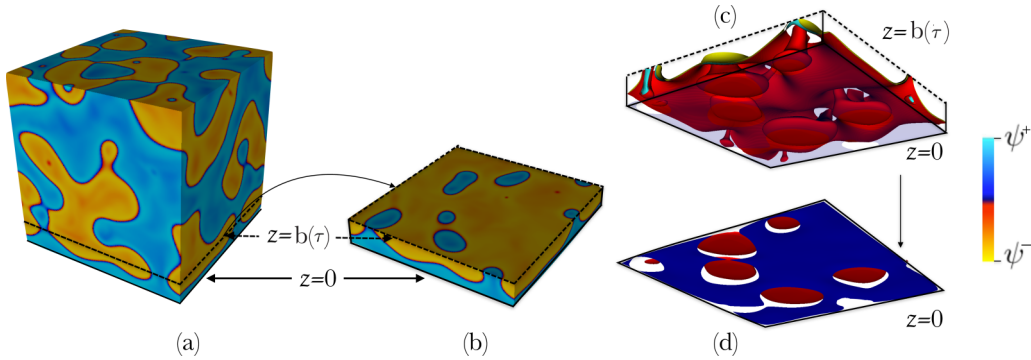


FIG. 4. Morphology of the fluid mixture at dimensionless time $\tau = 20$ (a) in the full computational domain with preferential wetting substrate at the bottom, and (b) in a slice of that domain up to a distance $z = 36$ from substrate that coincides with the plane $z = b(\tau)$ in Fig. 1. The slice shows the width of the *tubes* in the depletion layer. (c) The isosurfaces visualise the internal morphology in the volume between $z = 0$ and $z = b(\tau)$. (d) In-plane morphology at $z = 0$, colored by the maximum, ψ^+ , minimum, ψ^- , values of the order parameter in that plane at time τ .

further away from the substrate and also rich in the preferred fluid. See also the morphology in the middle row and middle column of Fig. 2. Once this layer breaks, we find a faster dynamics to occur. At even later times, the depletion layer also breaks up, as can be seen in the middle row and right most column of Fig. 2. When this happens, direct contact of the wetting layer with the bulk mixture is established. This leads to an even faster growth of the wetting layer thickness with what appears to be an exponent much larger than unity, accelerated presumably by hydrodynamic transport driven by curvature of the interface or gradients in interfacial tension. Eventually, similar to the prequench state close to the critical point, an exponent of unity is reached in the very late stages of demixing.

It seems that the structure of the depletion layer dictates at what rate the wetting layer thickness grows. Depending on whether there is an intact depletion *layer*, or a depletion *zone* in which tubes of the secondary wetting layer penetrate the depletion layer, decides by what mechanism the wetting layer thickness increases. If the depletion layer is intact, which is the case for $\alpha = 0$ for all times and for $\alpha = 1$ during the early stages, then growth of the wetting layer is slow because the wetting component has to diffuse through the depletion layer. The depletion layer is for that component a thermodynamically unfavourable layer dominated by the nonwetting component, and hence represents a free energy barrier for diffusion through it. When the depletion layer finally breaks and a depletion zone is created, the transport of material from the secondary wetting layer to the wetting layer is no longer faced by a free energy barrier, and only limited by the number and width of the *tubes* passing through it.

Furthermore, in the late stages of demixing, for $\alpha = 100$ we notice in Fig. 3 that the growth exponent decreases below unity, only to increase to the expected value of unity again. As we shall see, this is a result of the flow of the preferred fluid through the tubes in the depletion layer that causes significant in-plane concentration variations next to the substrate. Moreover, this deceleration is not to $\alpha = 100$, see the decrease in the growth exponent for $\alpha = 25$ close to $\tau = 20$.

In order to delve more deeply into the impact of the morphology of the depletion layer, we sketch in Fig. 1 the

order parameter field $\psi(x, y, z)$ at a time τ and a particular height z , the maximum and minimum values of which are indicated by ψ^+ and ψ^- . To estimate the characteristic length scale normal to the substrate, we average the order parameter laterally over each plane parallel to the substrate resulting in an order-parameter profile $\bar{\psi}$, which is a function of time τ and distance z from the substrate. As already discussed, the concentration wave that develops after some time exhibits an alternating layering induced by the surface interaction. The preferred fluid accumulates next to the substrate, increasing its amplitude $a(\tau) = \psi(0, \tau)$ with time until it attains an equilibrium value that depends on the quench depth and the strength of the surface interaction. The normal length scale or wetting layer thickness, L_{\perp} , however, keeps on growing with time as the concentration wave propagates into the bulk.

The depletion layer next to the wetting layer moves away from the substrate in tandem with the wetting layer widening. If tubes at some point penetrate the depletion layer, then the width of these tubes turn out to be the smallest in the plane halfway between the first and second zero crossings of the order parameter, positioned at $z = b(\tau)$ in Fig. 1. This can actually be clearly seen in Fig. 4. Note that as the concentration wave front propagates into the bulk, the position of the center of the depletion zone $b(\tau)$ increases. In this plane, the concentration of the nonpreferred fluid is the largest. It stands to reason that the precise morphology of the fluid around this plane must be significant in the evolution kinetics of the wetting layer thickness.

Focusing attention on the three-dimensional structure of the wetting layer and that of the depletion zone, Fig. 4 shows the morphology between the planes $z = 0$ and $z = b(\tau)$, visualized as isosurfaces of different densities. The figure shows that fluid transported from the secondary wetting layer through the tubes in the depletion layer spreads out toward the substrate, giving the iso-surface of this material transport the impression of inverted mushrooms. The density profiles showed in the top and the bottom of this three-dimensional visualisation correspond to the profiles in the planes $z = b(\tau)$ and $z = 0$, respectively. We measured the in-plane length scale L_{\parallel} in the middle of the depletion zone at $z = b(\tau)$, and find that the growth of this length scale, which represents the

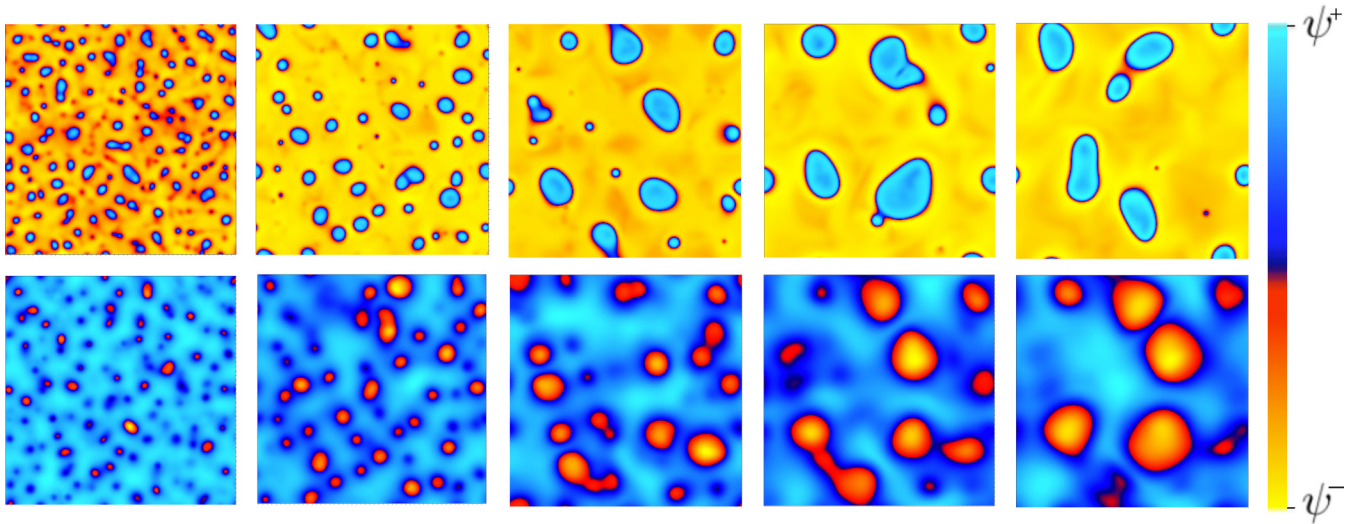


FIG. 5. Temporal evolution of in-plane density fields for $\alpha = 100$ at the dimensionless times $\tau = 4, 8, 12, 16,$ and 20 going from left to right. Shown are cross sectional morphologies of the mixture at the plane halfway between first and second zero crossing of the in-plane averaged order parameter (top row), so at a position $z = b(\tau)$ from the substrate, and that next to the substrate at $z = 0$ (bottom row). See also Fig. 1. The density fields are scaled to the maximum and minimum values of density ψ^+ and ψ^- in each plane for each time to highlight the concentration variation in the fluid layer next to the substrate and the smallest width of the tubes passing through the depletion layer. See the main text for definitions.

smallest width of the tubes, closely matches that of a bulk system. Thus, although the normal and in-plane length scales dictate the dynamics close to the substrate, we find that the relevant in-plane length scale, in fact, follows bulk behavior.

More information on the structure of the wetting layer and depletion zone is given in Figs. 5 and 6, showing the in-plane density distribution at positions $z = b(\tau)$, in the middle of the first depletion layer, and $z = 0$, next to the substrate, for different times τ . We scaled the density fields to the maximum and minimum value of density, ψ^+ and ψ^- for each time, to

highlight the concentration variations in the fluid layer next to the substrate and the shape of the smallest cross-sections of the tubes in the depletion zone. The absolute values of the maximum and minimum value of density, ψ^+ and ψ^- for each time shown in Figs. 5 and 6 are also shown in Fig. 7.

We see in Fig. 5 that for a prequench state close to the critical point, there are *holes* in the depletion layer from the early times on. These *holes* have the smallest width of the *tubes* passing through the depletion layer, as already announced. The fluid flowing through these tubes must be driven by

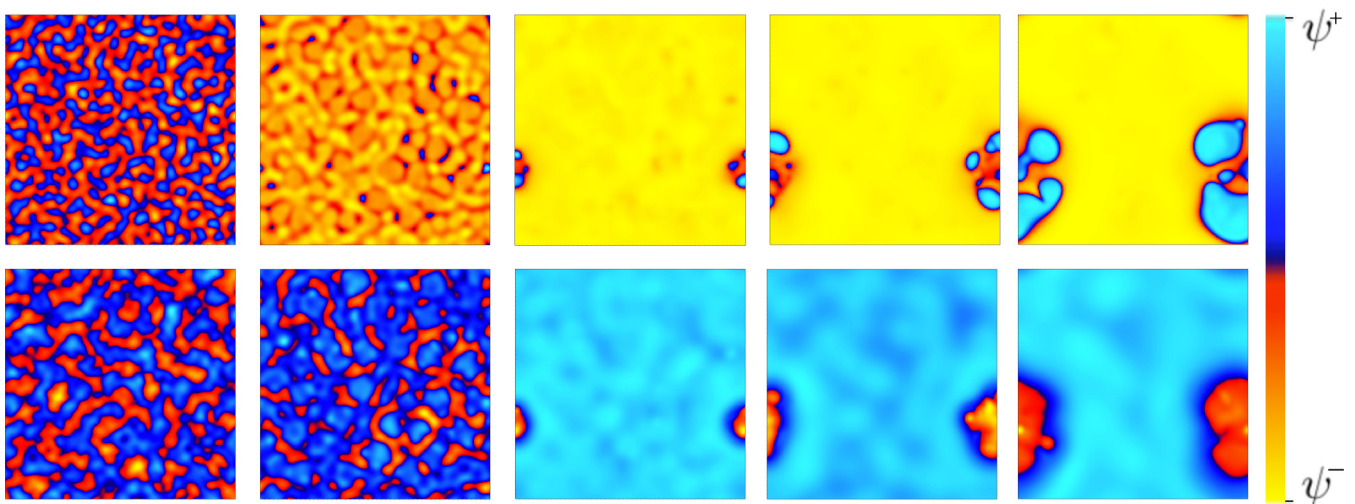


FIG. 6. Temporal evolution of in-plane density field for $\alpha = 1$ at the times $\tau = 4, 8, 12, 16,$ and 20 , going from left to right. Shown are cross sectional morphologies of the mixture at the plane halfway between first and second zero crossing of the in-plane averaged order parameter (top row), so at a position $z = b(\tau)$ from the substrate, and next to the substrate at $z = 0$ (bottom row). See also Fig. 1. The density fields are scaled to the maximum and minimum values of density ψ^+ and ψ^- in each plane for each time (reported in Fig. 7), to highlight the concentration variation in the fluid layer next to the substrate and the smallest width of the tubes passing through the depletion layer. The time, τ , is the simulation time scaled by the spinodal time scale for bulk mixtures initiated with $\alpha = 100$. See the main text for definitions.

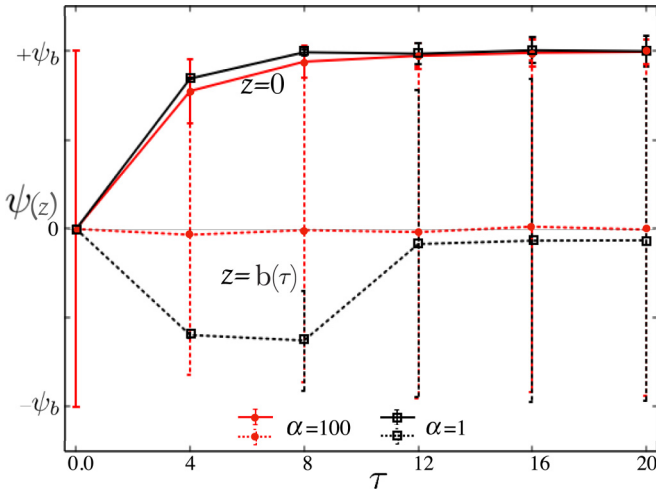


FIG. 7. In-plane order parameter $\psi(z)$ as a function of scaled time τ for initial concentration fluctuation amplitudes $\alpha = 1$ (red circles) and $\alpha = 100$ (black squares), at the substrate for $z = 0$ (solid lines) and midway in the depletion layer for $z = b(\tau)$ (dashed lines). The bars indicate the values of the maximum and minimum values ψ^+ and ψ^- from Figs. 5 and 6. See also the main text. Note that in component B -rich regions we have $\psi > 0$, while in component A -rich regions $\psi < 0$.

hydrodynamic effects arguably caused by curvature of the interface and possibly also by gradients in the interfacial tension [44]. This leads to flow of material directly from the secondary wetting layer to the wetting layer next to the substrate at $z = 0$, causing large in-plane concentration variations.

In contrast, for an initial state away from the critical point, shown in Fig. 6, the holes start to slowly form in the depletion layer and then only at late times. Unlike the in-plane morphology of $z = b(\tau)$ and 0 for a prequench state close to the critical point, we notice that there are only minor concentration variations in the early stages of phase separation. Notice in the right-most three panels the formation of a hole in the depletion layer at $\tau = 8$, and the corresponding influx of the material into the wetting layer at $z = 0$. The width of these holes, again, turns out to match the growth of the prevalent length scale in an equivalent bulk fluid.

The more profound impact concentration fluctuations have for the wetting layer at $z = 0$ can actually be seen in late stages of demixing, when in spite of being in direct contact with the bulk there actually is a *deceleration* in the growth of the wetting layer thickness for $\alpha = 100$. This is caused by the circumstance that the fluid that rushes into the wetting layer has much lower concentration of the wetting component than the average contact value of the order parameter, $a(\tau)$. Hence, because of this the growth of the wetting layer thickness must slow down. This in fact is clearly visible in Fig. 3. The size of the cross-section tubes in the depletion zone around the plane $z = b(\tau)$ grows consistently when $\alpha = 100$.

In contrast, if the prequench state is away from the critical point, and $\alpha = 1$, tubes start to form later on and hence we find that the corresponding concentration fluctuations at $z = 0$ only become significant at much later times. In that case, the composition develops an oscillatory profile and an intact depletion layer in the early stages of demixing. Much later,

bulk phase separation interferes with the oscillatory profile and only the wetting layer survives. Moreover, we see from Fig. 7 that the fluid layer next to the substrate at $z = 0$ remains rich in the preferred fluid B from early times on for both small and large initial concentration variations. This is indicated by the extremities of the bar that denote the maximum and minimum values of the in-plane concentration variations ψ^+ and ψ^- , both of which have a value larger than zero for the fluid layer at $z = 0$ at all times τ plotted in Fig. 7. However, as we saw in Fig. 6, the fluid in the depletion layer at $z = b(\tau)$ is rich in fluid A only during early times, and approaches the $\psi = 0$ -line in the late stages, signifying a transition from an intact depletion layer to a depletion zone riddled by tubes rich in B that connect to the wetting layer.

IV. CONCLUSIONS

In this paper, we investigate by means of lattice Boltzmann simulations the profound impact of the thermodynamic state of a symmetric binary mixture has prior to a quench in the spinodal region on the morphology and growth dynamics in surface-directed spinodal decomposition. Our aim in particular is to elucidate the role of spontaneous concentration fluctuations in the prequench state of the mixture. A large amplitude of concentration fluctuations implies a prequench state close to the critical point, and a small amplitude one that is not all too close to it. For simplicity we ignore in our simulations spatial correlations between these concentration variations immediately before the sudden change in thermodynamic conditions.

We find that concentration fluctuations interfere with the spinodal concentration wave that develops early in the process of phase separation near a substrate that is preferentially wet by one of the components, and hence that the prequench state does indeed impact upon the phase ordering kinetics near a surface. This is particularly true for coarsening processes along the normal to the substrate, but less so in the plane of the substrate where coarsening seems to be similar to that far away in for the substrate in the bulk of the fluid. We argue that the in-plane length scale in a sense mirrors the bulk length scale.

Focusing on the wetting layer thickness that we identify as relevant length scale normal to the substrate, we recover the diffusive scaling exponent of one-third for large initial concentration fluctuations crossing over to unity in the very late stages of coarsening. However, for relatively weak but nonzero initial concentration fluctuations, we find a growth exponent of the wetting layer thickness closer to one-fourth than to one-third, crossing over to unity again much later in time. This, we attribute to the stratification of alternate layers of preferred and nonpreferred fluids next to the substrate that is destroyed when the fluctuations are sufficiently large.

We find that the morphology of the depletion layer, rich in the nonpreferred fluid, is crucial to the dynamics in surface-directed spinodal decomposition. As long as the depletion layer remains intact, diffusion is slow. After breaking, tubes of the wetting phase pass through it and speed up the widening of the wetting layer. For large initial concentration fluctuations, stratification is by and large destroyed from the early stages of the demixing on, and tubes penetrating the depletion layer

connect the wetting layer with the bulk. These tubes facilitate faster growth of the wetting layer.

In the later stages of demixing, we actually find a deceleration in the growth of the wetting layer and a growth exponent smaller than unity. This we attribute to the flow of fluid from bulk to the wetting layer through the tubes, resulting in significant in-plane concentration variation in the wetting layer and in dropletlike structures with a lower concentration of the wetting component near the substrate.

Despite the fact that the problem of surface-directed phase transitions has attracted significant attention, many unresolved problems remain. For instance, how fluctuations impact phase ordering near a surface if the mixture has an off-critical composition should be of interest, as is what the effect is of the spatial correlation in the prequench state and the subsequent solidification resulting in the final morphology, e.g., in practical applications of organic photovoltaics. It would also be interesting to study the dependence of the growth exponent on film thickness for neutral top boundary and when the top boundary is also preferentially wet by a fluid component. In fact, our simulations presume Newtonian fluid dynamics, even though in practice the fluids often contain polymers that behave visco-elastically. In any event, we believe that the *prequench state* of the mixture may well be used to tailor the morphologies of functional thin film materials.

ACKNOWLEDGMENTS

This research was funded by the Institute branch of Netherlands Organisation for Scientific Research (NWO) and Royal Dutch Shell under the programme Computational Sciences for Energy Research (CSER) with Project No. 15CSER016.

APPENDIX A: LATTICE BOLTZMANN METHOD

We generate three-dimensional blended morphologies formed during spontaneous demixing in bulk and on a wetting substrate using the lattice Boltzmann (LB) model [37,38]. The lattice Boltzmann equation is derived from spatially and temporally discretizing the Boltzmann equation. The lattice Boltzmann method models fluid flow at mesoscopic level in terms of single particle distribution function $f_i(\mathbf{x}, t)$ at positions \mathbf{x} and time step t . The distribution function evolves as particles stream (LB terminology for “move”) and collide with each other as described by the discretized LB equation

$$f_i(\mathbf{x} + \mathbf{e}_i \Delta t, t + \Delta t) - f_i(\mathbf{x}, t) = -\frac{\Delta t}{\tau} [f_i(\mathbf{x}, t) - f_i^{\text{eq}}(\mathbf{x}, t)], \quad (\text{A1})$$

where \mathbf{e}_i is the i th microscopic velocity on the lattice and $f_i(\mathbf{x}, t)$ is the corresponding single-particle distribution function. The term τ is a relaxation time toward a equilibrium distribution function $f_i^{\text{eq}}(\mathbf{x}, t)$, and links to the viscosity of the fluid through the relation $\nu = c_s^2(\tau - \Delta t/2)$. $f_i^{\text{eq}}(\mathbf{x}, t)$ is the equilibrium Maxwell-Boltzmann distribution, truncated at the second order in velocity

$$f_i^{\text{eq}}(\mathbf{x}, t) = \rho \omega_i \left[1 + \frac{\mathbf{u}_{\text{eq}} \cdot \mathbf{e}_i}{c_s^2} + \frac{1}{2} \left(\frac{\mathbf{u}_{\text{eq}} \cdot \mathbf{e}_i}{c_s^2} \right)^2 - \frac{\mathbf{u}_{\text{eq}} \cdot \mathbf{u}_{\text{eq}}}{2c_s^2} \right]. \quad (\text{A2})$$

Here, $c_s = \frac{1}{\sqrt{3}} \frac{\Delta x}{\Delta t}$ is the lattice speed of sound and ω_i is a direction-dependent weight factor. The fluid density and velocity fluctuations are obtained by taking zeroth and first moments of the distribution function over the discrete lattice velocity space. Mathematically, $\rho(\mathbf{x}, t) = \rho_r \sum_i f_i(\mathbf{x}, t)$, where ρ_r is a reference density, and $\mathbf{u}(\mathbf{x}, t) = \sum_i f_i(\mathbf{x}, t) \mathbf{e}_i / \rho(\mathbf{x}, t)$. The pressure and the density fluctuations are related by a linearized ideal gas equation of state $p(\mathbf{x}, t) = c_s^2 \rho(\mathbf{x}, t)$.

For a binary mixture with fluid components A and B , two single-particle distribution functions $f_i^A(\mathbf{x}, t)$ and $f_i^B(\mathbf{x}, t)$ are used. The corresponding fluid densities are defined as $\rho^A(\mathbf{x}, t) = \rho_r \sum_i f_i^A(\mathbf{x}, t)$, $\rho^B(\mathbf{x}, t) = \rho_r \sum_i f_i^B(\mathbf{x}, t)$, and the velocities are defined as $\mathbf{u}^A(\mathbf{x}, t) = \sum_i f_i^A(\mathbf{x}, t) \mathbf{e}_i / \rho^A(\mathbf{x}, t)$ and $\mathbf{u}^B(\mathbf{x}, t) = \sum_i f_i^B(\mathbf{x}, t) \mathbf{e}_i / \rho^B(\mathbf{x}, t)$, respectively. The velocity in the equilibrium distribution function is $\mathbf{u}_{\text{eq}} = (\rho^A \mathbf{u}^A + \rho^B \mathbf{u}^B) / (\rho_A + \rho_B)$.

Throughout this work, we utilize two components A and B such that $\tau^A = \tau^B$. We use a D3Q19 lattice, which is a three-dimensional lattice with 19 discrete velocities. For brevity and numerical efficiency, we choose the lattice constant Δx , the time step Δt , the unit mass ρ_r to be unity. Furthermore, we introduce the interaction between the fluid components through a pseudopotential interaction force proposed by Shan and Chen [39],

$$\mathbf{F}^A(\mathbf{x}, t) = -G^{AB}(\mathbf{x}) \rho^A(\mathbf{x}, t) \sum_i \omega_i \rho^B(\mathbf{x} + \mathbf{e}_i, t) \mathbf{e}_i. \quad (\text{A3})$$

This force is a nearest-neighbor interaction term between fluid components A and B and is scaled through the choice of the parameter G^{AB} . This force is applied to the fluid by adding a shift of $\Delta \mathbf{u}^A(\mathbf{x}, t) = \frac{\tau^A \mathbf{F}^A(\mathbf{x}, t)}{\rho^A(\mathbf{x}, t)}$ to $\mathbf{u}_{\text{eq}}(\mathbf{x}, t)$ during a collision. Similar force and velocity term $\mathbf{F}^B(\mathbf{x}, t)$ and $\Delta \mathbf{u}^B(\mathbf{x}, t)$ is obtained for the fluid component B . This model results in phase separation of the two fluids, and the formation of a diffuse interface between them.

As we model phase separation in the vicinity of a wall (or substrate), the contact angles and their implications must be correctly represented. This determines the fluid-wall interaction and the relative preference of either components for contact with the substrate. In the lattice Boltzmann method, wall boundaries can be combined with the pseudopotential interaction. For a binary mixture with components A and B , the interaction force, following the pseudopotential method presented by Shan and Chen, can be incorporated in the description by an interaction force with the wall boundary nodes (s) as [40,41]

$$\mathbf{F}^{sA} = -G^{sA}(\mathbf{x}) \rho^A(\mathbf{x}) \sum_i s(\mathbf{x} + \mathbf{e}_i) \mathbf{e}_i, \quad (\text{A4})$$

where $s(\mathbf{x} + \mathbf{e}_i)$ is 1 if $(\mathbf{x} + \mathbf{e}_i)$ is a wall boundary node, and 0 if it is not. Here, $G^{sA}(\mathbf{x})$ is an interaction strength parameter for every component A and B . The surface interaction strength, φ , represents the relative wetting parameter $G^{sB} - G^{sA}$. The surface tensions γ^{sA} , γ^{sB} , and γ^{AB} are linearly proportional to the corresponding interaction parameter, and the equilibrium contact angle can thus be determined from these interaction parameters.

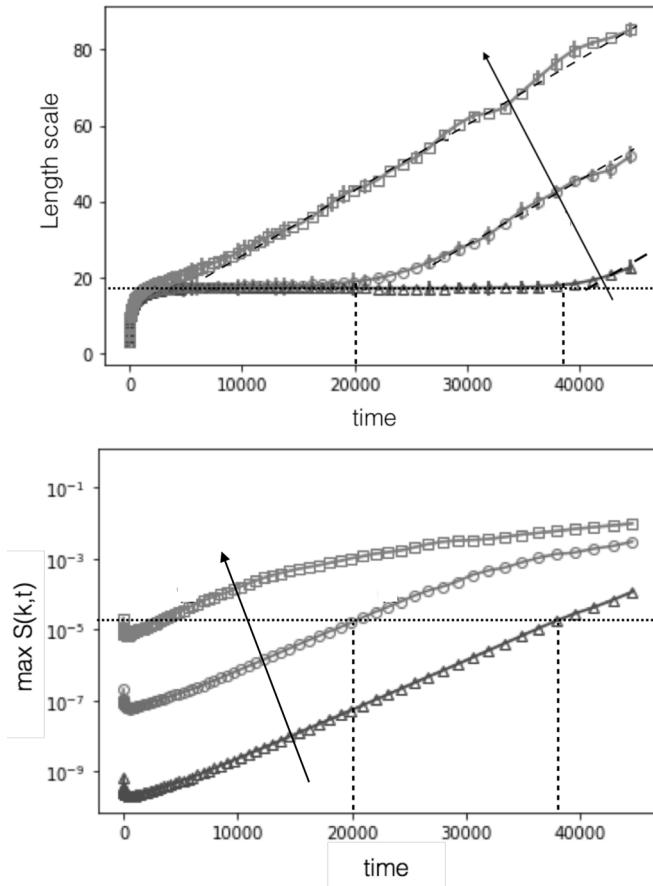


FIG. 8. Time evolution of the prevalent length scale (top) and maximum of the structure factor (bottom) of a symmetric fluid mixture AB undergoing phase separation by spinodal decomposition in bulk from an initially well-mixed state. Indicated are results for initial concentration fluctuation amplitudes $\alpha = 1$ (triangles), 10 (circles), and 100 (squares), with the arrow indicating increasing values of α . Domain growth in bulk remains isotropic for all values of α . The magnitude of the initial density fluctuations controls the temporal evolution of the fluid mixture and departure from spinodal decomposition. The dashed vertical lines indicate the transition time from spinodal decomposition to coarsening. Time is measured in the usual LBM units.

We keep the strength of surface interaction at the bottom wall, $\varphi = 0.3$, for which component B wets the substrate. Although this corresponds to partial wetting for a sessile drop of the B phase on a substrate, however, the finite size of the domain in our simulations and condensation of material next to the substrate leads to complete wetting of the substrate for the strengths of surface interaction modeled.

APPENDIX B: IMPACT OF THE AMPLITUDE OF THE INITIAL SPATIAL DENSITY FLUCTUATION IN BULK

We find that in *bulk*, large initial concentration fluctuations accelerate the demixing process, leading to isotropic coarsening from early times on. The bulk dynamics is thus characterized by a single length scale that we estimate from the position of the peak of the three-dimensional structure factor. As reported in the experimental studies for various pre-

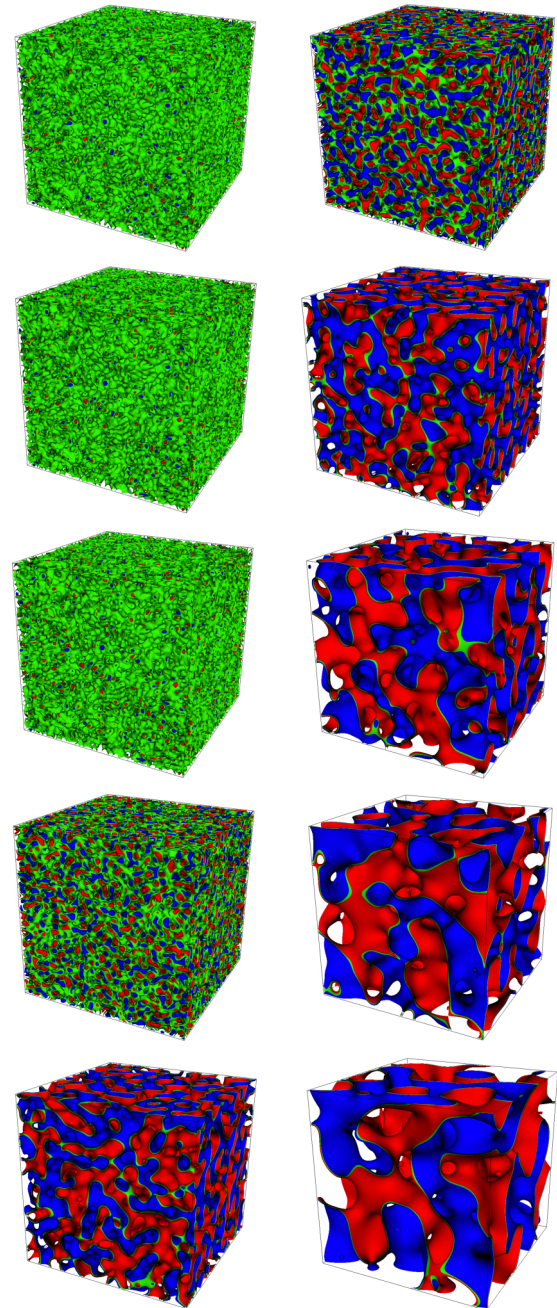


FIG. 9. Time evolution of the morphology resulting from the phase separation of a symmetric AB fluid mixture with small, $\alpha = 1$ (left column), and large, $\alpha = 100$ (right column), initial concentration fluctuations. Snapshots are taken at simulation time steps $t = 10\,000$, $20\,000$, $30\,000$, $40\,000$, and $50\,000$ from top to bottom. The two phases in the phase separating mixture are represented by red and blue isosurfaces, whereas the interface between the two is shown in green. Notice that the domain grows isotropically independent of the prequench fluctuation state of the mixture. The spinodal time following which coarsening initiates, we find to depend on the prequench state. See also Fig. 8.

quench states of the bulk mixture [15], the growth exponents associated with the coarsening that we find turn out to not depend on the corresponding amplitude of the concentrations fluctuations in the initial state. Figure 8 shows that the growth

exponents associated with coarsening in bulk remain independent of the amplitude of the concentration fluctuations at zero time, as expected. Note that the peak of the structure factor, denoted by “ $\max S(k, t)$ ” in Fig. 8, first decreases before increasing again because each lattice site in the simulation box is initialized with values $\pm\psi_0$, randomly distributed over the simulation box. This generates sharp interfaces at time $t = 0$, which are strongly penalized in the simulations at very very early times. This however, does not influence the phase order kinetics modeled, and the peak of the structure factor increases again after the initial decrease.

As we see in from the bulk lengthscale in Fig. 8, independent of the amplitude of the initial concentration fluctuations, the demixing initiates via the spinodal regime, wherein the peak in the structure factor initially remains stationary at a characteristic wave number, after which it shifts toward lower values. This then demarcates the commencement of coarsening, leading to domain growth with an exponent of unity. The same is true for the morphology, showing that the amplitude of the initial concentration fluctuations that we use to describe the equilibrium fluctuations in the prequench state does not alter the structure of the demixing fluid; see Fig. 9.

-
- [1] J. S. Higgins and J. T. Cabral, A thorny problem? Spinodal decomposition in polymer blends, *Macromolecules* **53**, 4137 (2020).
- [2] W. Hou, Y. Xiao, G. Han, and J.-Y. Lin, The applications of polymers in solar cells: A review, *Polymers* **11**, 143 (2019).
- [3] L. X. Chen, Organic solar cells: Recent progress and challenges, *ACS Energy Lett.* **4**, 10 (2019).
- [4] K.-M. Huang, Y. Q. Wong, M.-C. Lin, C.-H. Chen, C.-H. Liao, J.-Y. Chen, Y.-H. Huang, Y.-F. Chang, P.-T. Tsai, S.-H. Chen *et al.*, Highly efficient and stable organic solar cell modules processed by blade coating with 5.6% module efficiency and active area of 216 cm², *Progr. Photovolt.: Res. Appl.* **27**, 264 (2019).
- [5] J. J. van Franeker, D. Westhoff, M. Turbiez, M. M. Wienk, V. Schmidt, and R. A. J. Janssen, Controlling the dominant length scale of liquid–liquid phase separation in spin-coated organic semiconductor films, *Adv. Funct. Mater.* **25**, 855 (2015).
- [6] O. Wodo and B. Ganapathysubramanian, Modeling morphology evolution during solvent-based fabrication of organic solar cells, *Comput. Mater. Sci.* **55**, 113 (2012).
- [7] E. D. Siggia, Late stages of spinodal decomposition in binary mixtures, *Phys. Rev. A* **20**, 595 (1979).
- [8] A. Onuki, Late stage spinodal decomposition in polymer mixtures, *J. Chem. Phys.* **85**, 1122 (1986).
- [9] T. Koga and K. Kawasaki, Late stage dynamics of spinodal decomposition in binary fluid mixtures, *Physica A* **196**, 389 (1993).
- [10] S. W. Koch, R. C. Desai, and F. F. Abraham, Dynamics of phase separation in two-dimensional fluids: spinodal decomposition, *Phys. Rev. A* **27**, 2152 (1983).
- [11] E. Velasco and S. Toxvaerd, Computer simulation of late-stage growth in phase-separating binary mixtures: Critical and off-critical quenches, *J. Phys.: Condens. Matter* **6**, A205 (1994).
- [12] M. K. Hazra, S. Sarkar, and B. Bagchi, Three-stage phase separation kinetics in a model liquid binary mixture: A computational study, *J. Chem. Phys.* **150**, 144501 (2019).
- [13] W. R. Osborn, E. Orlandini, M. R. Swift, J. M. Yeomans, and J. R. Banavar, Lattice Boltzmann Study of Hydrodynamic Spinodal Decomposition, *Phys. Rev. Lett.* **75**, 4031 (1995).
- [14] G. Gonnella, E. Orlandini, and J. M. Yeomans, Spinodal Decomposition to a Lamellar Phase: Effects of Hydrodynamic Flow, *Phys. Rev. Lett.* **78**, 1695 (1997).
- [15] H. Jinnai, H. Hasegawa, T. Hashimoto, and C. C. Han, Time-resolved small-angle neutron scattering study of spinodal decomposition in deuterated and protonated polybutadiene blends. I. Effect of initial thermal fluctuations, *J. Chem. Phys.* **99**, 4845 (1993).
- [16] R. A. L. Jones, L. J. Norton, E. J. Kramer, F. S. Bates, and P. Wiltzius, Surface-Directed Spinodal Decomposition, *Phys. Rev. Lett.* **66**, 1326 (1991).
- [17] M. Geoghegan and G. Krausch, Wetting at polymer surfaces and interfaces, *Prog. Polym. Sci.* **28**, 261 (2003).
- [18] G. Krausch, J. Mlynek, W. Straub, R. Brenn, and J. F. Marko, Order-induced period doubling during surface-directed spinodal decomposition, *Europhys. Lett.* **28**, 323 (1994).
- [19] S. Puri and Y. Oono, Effect of noise on spinodal decomposition, *J. Phys. A: Math. Gen.* **21**, L755 (1988).
- [20] S. Puri and H. L. Frisch, Surface-directed spinodal decomposition: Modeling and numerical simulations, *J. Phys.: Condens. Matter* **9**, 2109 (1997).
- [21] S. Puri, Surface-directed spinodal decomposition, *J. Phys.: Condens. Matter* **17**, R101 (2005).
- [22] K. Binder, Collective diffusion, nucleation, and spinodal decomposition in polymer mixtures, *J. Chem. Phys.* **79**, 6387 (1983).
- [23] G. Brown and A. Chakrabarti, Surface-directed spinodal decomposition in a two-dimensional model, *Phys. Rev. A* **46**, 4829 (1992).
- [24] S. Puri and K. Binder, Power Laws and Crossovers in Off-Critical Surface-Directed Spinodal Decomposition, *Phys. Rev. Lett.* **86**, 1797 (2001).
- [25] P. K. Jaiswal, S. Puri, and S. K. Das, Surface-directed spinodal decomposition: A molecular dynamics study, *Phys. Rev. E* **85**, 051137 (2012).
- [26] S. Bastea, S. Puri, and J. L. Lebowitz, Surface-directed spinodal decomposition in binary fluid mixtures, *Phys. Rev. E* **63**, 041513 (2001).
- [27] S. K. Das, S. Puri, J. Horbach, and K. Binder, Kinetics of phase separation in thin films: Simulations for the diffusive case, *Phys. Rev. E* **72**, 061603 (2005).
- [28] S. K. Das, S. Puri, J. Horbach, and K. Binder, Spinodal decomposition in thin films: Molecular-dynamics simulations of a binary lennard-jones fluid mixture, *Phys. Rev. E* **73**, 031604 (2006).
- [29] B. T. Jiang and P. K. Chan, Effect of concentration gradient on the morphology development in polymer solutions undergoing thermally induced phase separation, *Macromol. Theory Simul.* **16**, 690 (2007).
- [30] D. Beysens and Y. Jayalakshmi, Kinetics of phase separation under a concentration gradient, *Physica A* **213**, 71 (1995).

- [31] G. Santonicola, R. Mauri, and R. Shinnar, Phase separation of initially inhomogeneous liquid mixtures, *Industr. Eng. Chem. Res.* **40**, 2004 (2001).
- [32] A. M. Lacasta, J. M. Sancho, and C. Yeung, Phase separation dynamics in a concentration gradient, *Europhys. Lett.* **27**, 291 (1994).
- [33] K. R. Elder, T. M. Rogers, and R. C. Desai, Early stages of spinodal decomposition for the cahn-hilliard-cook model of phase separation, *Phys. Rev. B* **38**, 4725 (1988).
- [34] J. F. Marko, Influence of surface interactions on spinodal decomposition, *Phys. Rev. E* **48**, 2861 (1993).
- [35] I. M. Lifshitz and V. V. Slyozov, The kinetics of precipitation from supersaturated solid solutions, *J. Phys. Chem. Solids* **19**, 35 (1961).
- [36] M. Iwamatsu, Dynamics of condensation of wetting layer in time-dependent Ginzburg–Landau model, *J. Colloid Interface Sci.* **316**, 1012 (2007).
- [37] S. Succi, *The Lattice Boltzmann Equation: For Fluid Dynamics and Beyond* (Oxford University Press, Oxford, UK, 2001).
- [38] T. Krüger, H. Kusumaatmaja, A. Kuzmin, O. Shardt, G. Silva, and E. M. Viggen, *The Lattice Boltzmann Method* (Springer International Publishing, Berlin, 2017).
- [39] X. Shan and H. Chen, Lattice Boltzmann model for simulating flows with multiple phases and components, *Phys. Rev. E* **47**, 1815 (1993).
- [40] R. Benzi, M. Sbragaglia, S. Succi, M. Bernaschi, and S. Chibbaro, Mesoscopic lattice Boltzmann modeling of soft-glass systems: Theory and simulations, *J. Chem. Phys.* **131**, 104903 (2009).
- [41] R. Benzi, L. Biferale, M. Sbragaglia, S. Succi, and F. Toschi, Mesoscopic modeling of a two-phase flow in the presence of boundaries: The contact angle, *Phys. Rev. E* **74**, 021509 (2006).
- [42] M. Sbragaglia, R. Benzi, L. Biferale, S. Succi, and F. Toschi, Surface Roughness-Hydrophobicity Coupling in Microchannel and Nanochannel Flows, *Phys. Rev. Lett.* **97**, 204503 (2006).
- [43] C. Harrison, W. Rippard, and A. Cumming, Video microscope and elastic light scattering studies of fast-mode kinetics in surface-mediated spinodal decomposition, *Phys. Rev. E* **52**, 723 (1995).
- [44] A. Goyal, P. van der Schoot, and F. Toschi, Demixing in a thin fluid film in contact with a sub-strate: interplay between surface wetting and hydrodynamics (unpublished).
- [45] P. Perlekar, R. Benzi, H. J. H. Clercx, D. R. Nelson, and F. Toschi, Spinodal Decomposition in Homogeneous and Isotropic Turbulence, *Phys. Rev. Lett.* **112**, 014502 (2014).
- [46] L. D. Landau and E. M. Lifshits, *Fluid Mechanics* (Pergamon Press, Oxford, UK, 1959), Vol. 11.
- [47] R. Adhikari, K. Stratford, M. E. Cates, and A. J. Wagner, Fluctuating lattice Boltzmann, *Europhys. Lett.* **71**, 473 (2005).
- [48] M. Gross, R. Adhikari, M. E. Cates, and F. Varnik, Thermal fluctuations in the lattice Boltzmann method for nonideal fluids, *Phys. Rev. E* **82**, 056714 (2010).